

# 17 Field Emission Enhancement of Multiwalled Carbon Nanotubes Film by Thermal Treatment under UHV and in Hydrogen and Ethylene Atmospheres

L. Stobinski<sup>a,b,\*</sup>, C. S. Chang<sup>c</sup>, H. M. Lin<sup>a</sup> and T. T. Tsong<sup>c</sup>

<sup>a</sup>Tatung University, Taipei 104, Taiwan, ROC

<sup>b</sup>Institute of Physical Chemistry, Polish Academy of Sciences, 01-224 Warsaw, Kasprzaka 44/52, Poland

<sup>c</sup>Institute of Physics, Academia Sinica, Taipei 115, Taiwan, ROC

Recently, much effort has been devoted to fabricate carbon nanotubes (CNTs)-based field emission display, as a very promising, low-energy and cheap electronic device of the 21<sup>st</sup> century (Bonard *et al.* 2001, Choi *et al.* 2001, Kim *et al.* 2000, Murakami *et al.* 2000, Saito *et al.* 2000). Due to the CNTs' extreme properties, like high aspect ratio, good electrical and thermal conductivity, high melting point and mechanical strength, and also low chemical reactivity, they seem to be a very promising and ideal material for devices based on cold electron emission. In the near future, great effort needs to be made to develop mass production technology for efficient and stable carbon nanotubes cold electron field emission sources. It is also important to develop other, additional physical and/or chemical methods that would improve the emission properties of carbon nanotubes while reducing the currently applied high bias. The present paper describes an attempt at improving the emission properties of multiwalled CNTs (MWCNTs) film by annealing it in a UHV system and *in situ* in an hydrogen or ethylene atmosphere.

As-prepared, spaghetti-like, MWCNTs film (5x5 mm) was used in our experiments and was fabricated by the thermal CVD method using Fe film (70 nm) as a catalyst deposited on a Si substrate by bombardment of a pure iron target by ion Ar<sup>+</sup> beam. Next, the sample was moved through the air to the thermal CVD system where it was heated in an H<sub>2</sub> atmosphere (~760 Torr) for 5 min. at 900 °C with H<sub>2</sub> flow of 5 sccm. Then, the gas was changed for a mixture of N<sub>2</sub> and C<sub>2</sub>H<sub>4</sub> (760 Torr) with a flow ratio of 10:5 sccm, respectively. During the CNTs' growth the sample was maintained at 850 °C for 5 min. Figure 1 presents the SEM image of a cross-section of MWCNTs film with many protruding single carbon nanotubes with diameters of 30–60 nm. One can notice that many carbonaceous and catalyst particles are attached to the surface of the CNTs. The Raman spectrum of the

---

\* Corresponding author . Email: lstob@ichf.edu.pl; lstob50@hotmail.com

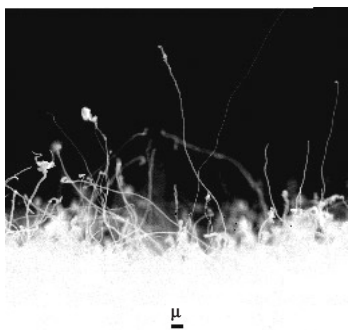


**Figure 1** Cross Section of MWCNTs film.

sample (514.5 nm) shows typical D ( $1346.0 \text{ cm}^{-1}$ ) and G ( $1577.5 \text{ cm}^{-1}$ ) modes (Choi *et al.* 2001). The field emission properties of the MWCNTs sample were studied in the UHV diode system with the gap about  $100 \text{ }\mu\text{m}$  between MWCNTs sample and ITO anode. The field emission current was measured at a pressure of  $10^{-9}$  Torr indicating at the very beginning high instabilities ( $\pm 200\%$ ). So, we decided to anneal the MWCNTs film to stabilize field emission by removing the water and other gaseous contaminations that could create current fluctuations. Since the same sample was used in several successive heating courses (maximum up to  $400 \text{ }^\circ\text{C}$ ), we

decided to use an electric field no higher than  $5 \text{ V}/\mu\text{m}$  to preserve the carbon nanotubes film in good condition for the next emission current measurements.

The first heating of the MWCNTs sample was carried out up to  $200 \text{ }^\circ\text{C}$  for 30 min at the pressure of  $10^{-8}$  Torr. After that, I-V curve during rise sweep was taken (Figure 2). Emission current fluctuations decreased up to about  $\pm 100\%$ . The average current density at  $5 \text{ V}/\mu\text{m}$  was  $0.85 \text{ mA}/\text{cm}^2$ . The turn-on field ( $E_{\text{to}}$ , calculated for  $10 \text{ }\mu\text{A}/\text{cm}^2$ ) and threshold field ( $E_{\text{thr}}$ , extrapolated for  $10 \text{ mA}/\text{cm}^2$ ) were  $2.8 \text{ V}/\mu\text{m}$  and  $6.6 \text{ V}/\mu\text{m}$ , respectively. The Fowler-Nordheim (F-N) model was used for the whole applied voltage range to present the tunneling electron field emission phenomena (Choi *et al.* 2001, Kim *et al.* 2000, Murakami *et al.* 2000, Saito *et al.* 2000). The F-N plot (Figure 3A) showed two different slopes of the straight line, indicating that under low and high bias the character of the field emission is changed. Taking the work function for carbon nanotubes as being equal to that for graphite,  $5 \text{ eV}$  (Bonard *et al.* 2001), we could calculate the field enhancement factors for the low and high electric field, i.e.,  $\beta_L \sim 15500$  and  $\beta_H \sim 41500$  with a change of the slope of the F-N plot at the breakpoint corresponding to the voltage,  $V_{\text{knee}} = 280 \text{ V}$ . The second heating of the MWCNTs sample up to  $300 \text{ }^\circ\text{C}$  for 1 hour was carried out under vacuum of  $10^{-7}$  Torr just after the first emission current measurement. Again, I-V curve during bias rise was measured under the pressure of  $10^{-9}$  Torr as shown in Figure 2. The fluctuations of the emission current decreased up to about  $\pm 50\%$ . The average current density at  $5 \text{ V}/\mu\text{m}$  was, similar as after the 1<sup>st</sup> annealing,  $0.78 \text{ mA}/\text{cm}^2$ .  $E_{\text{to}}$  and  $E_{\text{thr}}$  (extrapolated) were estimated for  $2.8 \text{ V}/\mu\text{m}$  and  $7.3 \text{ V}/\mu\text{m}$ , respectively. The F-N plot (Figure 3B) also presented two slopes of the liner dependence.  $\beta_L$  and  $\beta_H$  were calculated for about 11500 and 53500, respectively with  $V_{\text{knee}} = 285 \text{ V}$ . This heating cycle did not change the values of the emission current and  $V_{\text{knee}}$ . This could mean that the MWCNTs film was not enough well degassed and stabilized. The higher pressure ( $10^{-7}$  Torr) during this heating would confirm this. The third heating of the MWCNTs sample in vacuum was performed shortly after the emission current measurement. This time the sample was heated up to  $400 \text{ }^\circ\text{C}$  for 1 hour. At the very beginning of the heating cycle the pressure of the system rose up to  $10^{-6}$  Torr but later gradually decreased and reached  $10^{-8}$  Torr. When the sample was cooled down to room temperature the pressure of the system reached again  $10^{-9}$  Torr and I-V curve during the voltage rise was measured again (Figure 2).

The fluctuations of the emitted current decreased this time below the level of  $\pm 20\%$ . The average current density at  $5 \text{ V}/\mu\text{m}$  was about  $1.56 \text{ mA}/\text{cm}^2$ .  $E_{\text{to}}$  and  $E_{\text{thr}}$  (extrapolated) were calculated for  $3.1 \text{ V}/\mu\text{m}$  and  $6.4 \text{ V}/\mu\text{m}$ , respectively. The F-N plot (Figure 3C) was calculated and also showed two slopes of the linear dependence.  $\beta_L$  and  $\beta_H$  were calculated for about 14000 and 41500, respectively with  $V_{\text{knee}}=370 \text{ V}$ . This time the emission current increased almost 100% and the applied voltage for the low emission current range was extended about 90 V. After the 4<sup>th</sup> thermal sample treatment at  $400^\circ\text{C}$ , where the MWCNTs film was heated in an  $\text{H}_2$  atmosphere at the pressure of 0.1 Torr for 1 hour, the emission current increased about 11%, i.e., up to  $1.73 \text{ mA}/\text{cm}^2$  at  $5 \text{ V}/\mu\text{m}$  (Figure 2).  $E_{\text{to}}$  and  $E_{\text{thr}}$  (extrapolated) were estimated for  $3.1 \text{ V}/\mu\text{m}$  and  $6.1 \text{ V}/\mu\text{m}$ , respectively. The F-N plot (Figure 3D) again showed two slopes of the linear dependence.  $\beta_L$  and  $\beta_H$  were found as being equal to 15000 and 33500, respectively with the breakpoint at the knee voltage of 370 V. The 5<sup>th</sup> heating of MWCNTs film at  $400^\circ\text{C}$  for 1 hour in ethylene atmosphere at the pressure of 0.1 Torr caused that the emission current (Figure 2) again increased about 22% (up to  $2.12 \text{ mA}/\text{cm}^2$  at  $5 \text{ V}/\mu\text{m}$ ). The F-N plot (Figure 3E) also showed two slopes of the nearly perfect linear dependence with  $\beta_L$  and  $\beta_H$  calculated for about 15900 and 35000, respectively with  $V_{\text{knee}}=370 \text{ V}$ .

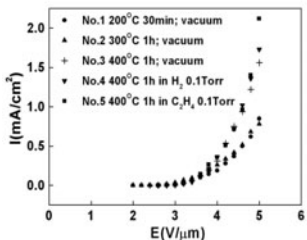


Figure 2

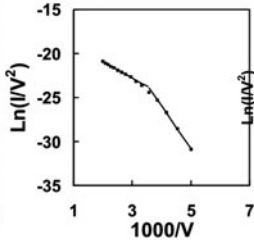


Figure 3A

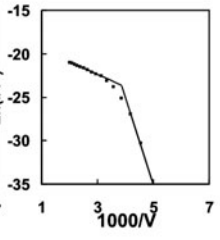


Figure 3B

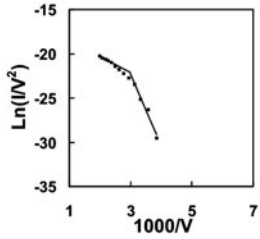


Figure 3C

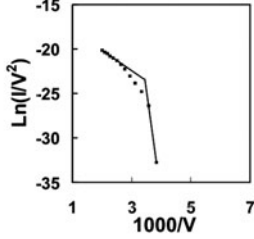


Figure 3D

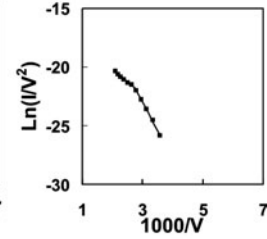


Figure 3E

Figure 2 I-V curves.

Figure 3 (A-E) Fowler-Nordheim plots.

In most papers on cold electron emission from CNTs, the linear dependence of the F-N plot for higher voltages, is usually seen to break down. In the F-N plots one can distinguish a low- and high-current region (Bonard *et al.* 2001, Choi *et al.* 2001, Kim *et al.* 2000, Murakami *et al.* 2000, Saito *et al.* 2000). It has been claimed that the range of the electron emission low current is correctly described by

the F–N plot, while the high-current, which is often also linear in the F–N coordinates, deviates from the F–N model. The usual explanation for this is that the high emission current lies within the saturation current range appearing due to the space-charge effect, and/or interaction between neighboring nanotubes emitters and/or gas desorption-adsorption on CNTs tips (Xu *et al.* 1999).

The linearity of the F–N plot within the higher-current region suggested that even in this region the current did not reach saturation. Thus, properties of CNTs under study might be satisfactorily described by the F–N model with varying either  $\beta$  and/or  $\phi$  parameters. This assumption implies a possibility of a change in the conditions of the electron field emission. If the F–N model describing the electron field emission from CNTs in the range below the saturation current is satisfactorily obeyed, only the quotient  $\phi^{3/2}/\beta$  describes the slope of the F–N plot. Reversible changes (perhaps with hysteresis) in  $\phi$  and/or  $\beta$  could also be anticipated. A declining F–N slope, then result from either a decrease in  $\phi$  or increase in  $\beta$ . Both parameters may change simultaneously in such manner that the quotient  $\phi^{3/2}/\beta$  effectively decreases. The temperature of the many nanotube emitters increases with increase in the strength of emission current (Joule heat). This temperature increase, particularly in the systems with high density of carbon nanotubes, is controlled by the equilibrium between generation and reception of heat from the whole CNTs emitter system. Undoubtedly, temperature of the CNTs tips increases significantly on electron emission and stabilizes at certain level. Thus, the CNTs emitters thermally elongate, and the thermal vibrations of carbon atoms in graphene sheets and the nanotubes intensify. Additional carbon sources of electron emission may also be generated and they also can contribute to increase in the effective electron enhancement factor,  $\beta$ . On increased electron emission at increased temperature of the carbon emitters, the work function of the carbon nanotubes emitters may also change. This could result from additional excited resonance in localized states and effectively reduce the CNTs work function. The emitting nanotube tips often carry small particles of catalyst. Any thermal and/or chemical treatment of CNTs may generate therein-chemical groups such as -H, -COOH, -CH<sub>3</sub>, -C<sub>2</sub>H<sub>5</sub>. During electron emission at higher temperatures, a modification of the nanotube tips may take place as the result of reaction with the desorbing/adsorbing gases. At lower temperature and at lower emission current, desorption of gases from CNTs almost ceases, and the original emission typical for non-completely degassed nanotubes can be noted. Because of the closed structure of the carbon nanotubes, their high aspect ratio, and when the UHV systems are not applied the fast and complete degassing of CNTs may be difficult. Therefore, over a long period of time many instances of similar changes in the value of emission current for different ranges of emission current can be observed. The  $\beta$  and  $\phi$  parameters take values dependent on applied voltage. Also after heating of CNTs film under either hydrogen or ethylene increased electron emission was observed. The most likely it resulted from decrease in the work function of the electron emitters and increase in the effective number of electron emitters, what could enlarge the  $\beta$  factor. In fact, under hydrogen at 400 °C a partial hydrogenation of the CNTs and particles of metal catalyst (here Fe), could be observed. It could lead to the formation of the CNT-H moieties and pure catalyst particles. After heating

CNTs in ethylene at 400 °C, clusters of amorphous carbon and a certain amount of newly formed CNTs appeared on the surface of the active catalyst particles. Moreover,  $\pi$ -complexes of CNTs with ethylene as well as products of addition ethylene to hydrogenated CNTs (CNT-CH<sub>2</sub>-CH<sub>3</sub> and CNT-(CH<sub>2</sub>-CH<sub>2</sub>)<sub>n</sub>-CNT) might be formed. In postulated  $\pi$ -complexes, ethylene fragment donated  $\pi$ -electrons to graphene reducing the carbon emitter work function, as shown by the results presented here. Also alkyl side-chains are known as electron donors by inductions as well as by resonance (Tomasik 2002).

Also another possible explanation for the breaking of the linearity of the F-N plot is that the finite resistance of a nanotube will likely cause a potential drop across it. It should be possible to derive the resistance from the curvature. We will look into this resistance effect in greater detail later.

For a better understanding of the phenomena of cold electron emission, many more experiments are necessary with pure and modified CNTs emitters. This would serve not only to explain the fundamental physical and chemical phenomena related to electron field emission from carbon nanotubes, but also has a practical aspect in terms of fabricating durable, stable and highly efficient carbon nanotube electron emitters working at lower and lower voltages.

## ACKNOWLEDGEMENTS

We would like to thank the National Science Council, Republic of China for financial support through Contract Number NSC 90-2811-E-036-001. The authors would like to thank Dr. K.H. Chen and Mr. C.H. Ling for help in the sample preparation, and Prof. P. Tomasik for the creative discussion.

## REFERENCES

- Bonard J. M., Kind H., Stockli T. and Nilsson L. O., 2001, Field emission from carbon nanotubes: the first five years. *Solid-State Electronics*, 45, pp. 893-914.
- Choi Y. C., Shin Y. M., Bae D. J., Lim S. C., Lee Y. H. and Lee B. S., 2001, Pattern growth and field emission properties of vertically aligned carbon nanotubes. *Diamond and Related Materials*, 10, pp. 1457-1464.
- Kim J. M., Choi W. B., Lee N. S. and Jung J. E., 2000, Field emission from carbon nanotubes for displays. *Diamond and related Materials*, 9, pp. 1184-1189.
- Murakami H., Hirakawa M., Tanaka C. and Yamakawa H., 2000, Field emission from well-aligned, patterned, carbon nanotube emitters. *Applied Physics Letters*, 76, pp. 1776-1778.
- Saito Y. and Sashiro U., 2000, Field emission from carbon nanotubes and its application to electron sources. *Carbon*, 38, pp. 169-182.
- Tomasik P., 2002, Department of Chemistry, Agriculture University, Cracow, Poland, private information.
- Xu X. and Brandes G. R., 1999, A method for fabrication large-area, patterned, carbon nanotube field emitters. *Applied Physics Letters*, 74, pp. 2549-2551.